14

Synthesis and Properties of Perfluorinated Polyimides

SHINJI ANDO, TOHRU MATSUURA, and SHIGEKUNI SASAKI

14.1. INTRODUCTION

14.1.1. Near-IR Light Used in Optical Telecommunication Systems

Silica-based single-mode optical fibers are used as the transmission medium in current optical telecommunication systems.[1] The transmission light is near-IR. Degradation of communication quality under transmission is minimized by using a 1.3 μm wavelength because the refractive index dispersion of these optical fibers is zero at this wavelength, which is thus called the zero-dispersion wavelength. On the other hand, this optical fiber has a minimum transmission loss at 1.55 μm. Techniques have been developed to shift the zero-dispersion wavelength of silica-based optical fibers to 1.55 μm. Future telecommunication subscriber systems will use both 1.3 and 1.55 μm as communication wavelengths[2] (e.g., 1.3 μm for communication service and 1.55 μm for one-directional video service).

The refractive index of the core of the optical fibers is made slightly higher than that of the cladding in order to confine the transmitted optical signals. A small amount of GeO_2 is doped into the core of the commonly used silica-based optical fibers in order to increase the refractive index. Since doping into the core is undesirable from the point of view of decreasing the transmission loss, fluorine is doped into the cladding of optical fibers to achieve very low transmission loss. The

use of fluorine decreases the refractive index of the medium and considerably decreases water absorption. The minimum loss of 0.154 dB/km at 1.55 μm obtained from a fluorine-doped optical fiber is close to the theoretical limit given by Rayleigh scattering and harmonic absorption of oxygen–hydrogen (O–H) and silicon–oxygen (Si–O) bond stretching.[3] The sharp absorption peak appearing at 1.38 μm is due to the second harmonic of the O–H bond stretching vibration of the residual Si–OH groups.[4] The optical communication wavelengths, 1.3 and 1.55 μm, are located in the valley between the absorption peaks and are called *windows.* This explains the very low transmission loss at these wavelengths.

14.1.2. Integrated Optics and Optical Interconnect Technology

With the advancement of optical telecommunication systems, "integrated optics" technology[5] and "optical interconnect" technology[6] are becoming more and more important. The major components of these two technologies are photonic integrated circuits (PICs), optoelectronic integrated circuits (OEICs), and optoelectronic multichip modules (OE-MCMs). All the functional devices, including optical and electronic components, are formed or attached to a single planar substrate. Optical signals are transmitted through optical waveguides that interconnect such components. The principle of optical transmission in wave-guides is the same as that in optical fibers. To implement these technologies, both active optical devices (such as light sources, optical switches, and detectors) and passive optical components (such as beam splitters, beam combiners, star couplers, and optical multiplexers) are needed. A wide variety of optical materials has been studied, e.g., glasses, lithium niobate, III-V semiconductors, and polymers. In particular, passive optical components have been fabricated using glass optical waveguides by ion-exchange,[7] or by flame hydrolysis deposition and reactive ion etching (FHD and RIE).[8] In the case of silica-based glass waveguides, all the waveguides and the passive optical components should be formed on the substrate before attaching the active optical and electronic devices because very high temperatures (up to 1300°C) are needed to consolidate silica when using FHD and RIE. In addition, the inflexibility of glass waveguides and the difficulty of processing large (longer than 30 cm) waveguides make it difficult to achieve PICs and OEICs. As a result, there has been a strong demand for materials for interconnecting waveguides and passive optical components that have high processability, flexibility, and the possibility of fabricating waveguides on the PICs, OEICs, or OE-MCMs after attaching or forming of optical and electronic components.

14.1.3. Polymeric Waveguide Materials for Integrated Optics

For the above reasons, polymers are expected to be used as waveguide materials for. optical interconnects and passive optical components on PICs; OEICs, and OE-MCMS.[9] The current manufacturing process for ICs and MCMs includes soldering at 270°C and brief processes at temperatures up to 400°C. Waveguide polymeric materials should therefore have high thermal stability, i.e., a high glass transition temperature (T_g) and a high polymer decomposition temperature as well as high transparency at the wavelengths of optical communications (1.3 and 1.55 μm).

Conventional polymeric materials used in plastic optical fibers and waveguides for short-distance optical datalinks, such as poly(methy1 methacrylate) (PMMA), polystyrene (PS), or polycarbonates, do not have such thermal stability. In addition, their optical loss at the wavelengths for optical communications are much higher than at visible wavelengths (0.4 ~ 0.8 μm), because carbon–hydrogen (C–H) bonds harmonically absorb near-IR radiation (0.8 ~ 1.7 μm). Figure 14.1 shows the visible–near-IR absorption spectrum of PMMA dissolved in chloroform with a concentration of 10 wt%. The influence of C–H bonds of chloroform was neutralized by using the same amount of chloroform as a reference. Two types of C–H bonds in PMMA, those in the methyl and methylene groups, give broad and strong absorption peaks in the near-IR region. Although 1.3 and 1.55 μm are located in the windows, absorption owing to C–H bonds increases the optical losses at these wavelengths.
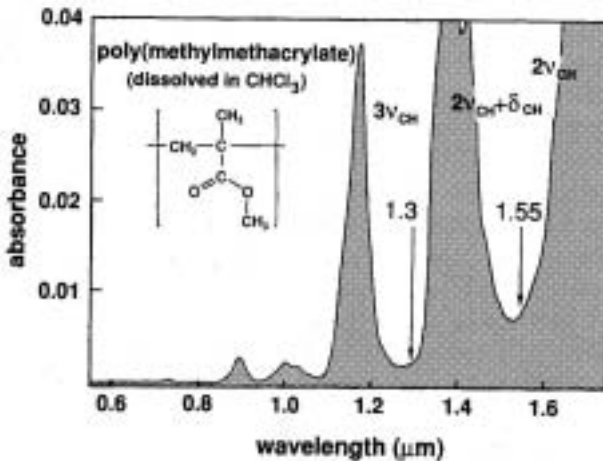

Figure 14.1. Visible–near-IR absorption spectrum of poly(methylmethacrylate) (PMMA) dissolved in chloroform. The same amount of chloroform was used as a reference (reproduced by permission of the American Chemical Society, from Ando et al.[28]).

Polyimides and epoxy resins have been investigated as optical waveguide materials because they have excellent thermal, chemical, and mechanical stability.[10–14] The first attempt to use polyimide for optical waveguides was made by Furuya *et al.*[10] They fabricated a laser–waveguide integration by using a spin-coated polyimide for the core layer of the waveguide. Franke and Crow[11] discussed the influence of the curing process of soluble polyimides and obtained an optical loss of less than 0.3 dB/cm at 0.633 μm. This loss is a measure of the change in the intensity of the light signal according to the following expression: dB = − 10 log(I/I_0). In this case, the loss per centimeter is approximately 7%. Sullivan[12] described polyimide waveguides fabricated by reactive etching. High-density router, splitter, and combiner building-block components have been developed in polyimide channel multimode waveguides. On the other hand, Hagerhorst-Trewhella *et al.*[13] reported solvent or wet-etching resist processes using UV-curable epoxies and polyimides with 0.3 dB/cm loss at 1.3 μm. Ablated mirrors using excimer lasers have been demonstrated for out-of-plane input/output interconnections. Reuter *et al.*[14] have reported that optimally cured partially fluorinated polyimides can be used to achieve optical losses below 0.1 dB/cm at visible wavelengths (at 0.63 μm), and that these losses are stable at temperatures up to 200°C and below 0.5 dB/cm up to 300°C.

14.1.4. Optical Transparency of Fluorinated Polyimides at Near-IR Wavelengths

The authors[15–17] demonstrated that single-mode embedded waveguides can be fabricated with fluorinated polyimides (see this volume, Chapter 15). To fabricate these single-mode waveguides, there must be precise control of the shape and size of the core and of the refractive indexes of the core and the cladding. The polyimides used are copolymers synthesized from pyromellitic dianhydride (PMDA) and 2,2-bis(3,4-dicarboxyphenyl)hexafluoropropane dianhydride (6FDA) as dianhydrides and 2,2'-bis(trifluoromethyl)-4,4'-diaminobiphenyl (TFDB) as a diamine.[18] The synthesis, properties, and optical applications of these partially fluorinated polyimides are described in Chapter 15. These waveguides have optical losses of less than 0.3 dB/cm at 1.3 μm.[16] The increase in optical loss was less than 5% after heating at 380°C for 1 h and at 85°C with relative humidity of 85% for over 200 h.[17] These materials also show high transparency at visible wavelengths as well as low dielectric constants, low refractive indexes, and low water absorption. In these properties, the materials are superior to those of conventional nonfluorinated polyimides and epoxies used for the waveguides described above.[19] Nonfluorinated polyimides have high water absorption of about 1.3–2.9 wt%,[20] which causes significant optical loss at 1.3 and 1.55 μm. Water molecules have strong absorption peaks in the near-IR region.[21]

However, fluorinated polyimides also have some absorption peaks in the near-IR region owing to C–H bonds in their phenyl groups. Figure 14.2 shows a schematic representation of the fundamental stretching bands and their harmonic absorption wavelengths for the carbon–hydrogen (C–H), carbon–deuterium (C–D), and carbon–fluorine (C–F) bonds. The wavelengths were measured for benzene, hexadeuterobenzene, and hexafluorobenzene with a near-IR spectro-photometer. For simplicity, the absorptions from the combinations of the harmonics and the deformation vibration are not shown, and the absorptions that are due to the fourth and fifth harmonics of the stretching vibration are negligibly small. The harmonics of C–D and C–F bonds are displaced to longer wavelengths than the C–H bond because the wavelengths for the fundamental stretching vibrations of C–D and C–F bonds are about 1.4 and 2.8 times longer than that of the C–H bond.

Since the absorption band strength decreases about one order of magnitude with each increase in the order of harmonics (i.e., the vibrational quantum number),[21] the losses at visible and near-IR wavelengths can be appreciably reduced by substituting deuterium or fluorine for hydrogen atoms. Kaino *et al.*[22,23] have produced low-loss optical fibers at visible wavelengths from deuterated
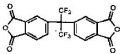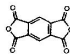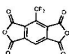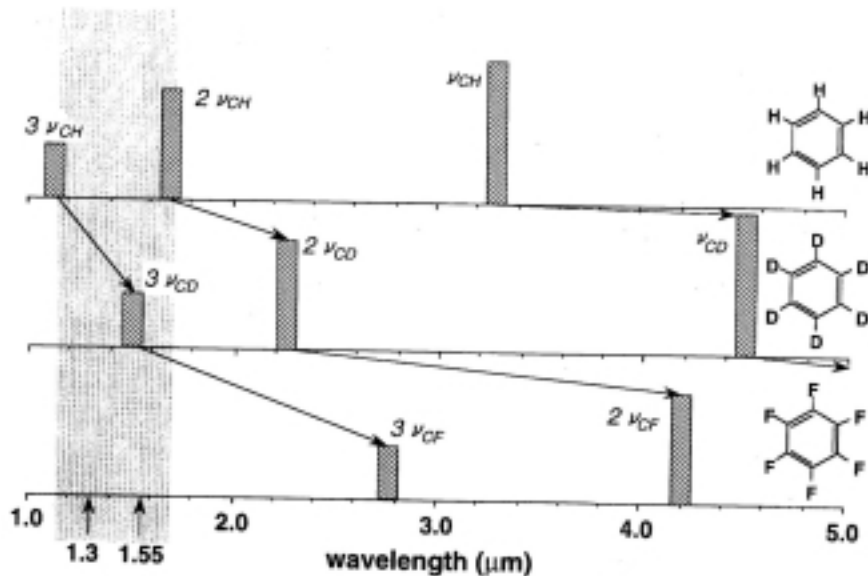

Figure 14.2. Schematic representation of fundamental stretching bands and their harmonic absorption wavelengths for C–H, C–D, and C–F bonds observed for benzene, hexadeuterobenzene, and hexafluorobenzene, respectively (reproduced by permission of the American Chemical Society, from Ando *et al.*[28]).

PMMAs and fluorodeuterated PSs. Imamura *et al.*[24] fabricated low-loss wave-guides of less than 0.1 dB/cm at 1.3 μm by using deuterated and fluorodeuterated PMMAs. This substitution has a significant effect in reducing the optical loss at visible wavelengths and 1.3 μm. However, the strength of the absorption due to the harmonics of C–D bond stretching appearing between 1.4 and 1.6 μm is not negligible at 1.55 μm. An automatic fiber line-testing system using a 1.65 μm wavelength as an identification signal is also being developed.[25] As can be seen in Figures 14.1 and 14.2, the transparency of conventional polymers having a C–H bond at 1.65 μm is extremely low because the second harmonics of C–H bond stretching is located at the same wavelength. Such polymers cannot be used in the optical components for the future telecommunication systems even if they are partially deuterated or fluorinated.

14.1.5. The Effect of Perfluorination on Optical Transparency

For the reduction of optical loss at near-IR wavelengths, perfluorination is, in principle, superior to perdeuteration. Table 14.1 shows the molecular structure and the properties of three kinds of existing perfluoropolymers, Teflon-AF (DuPont), Cytop (Asahi Glass Co.), and poly(tetrafluoroethylene) (PTFE). A semicrystalline polymer, PTFE cannot be used for light-transmitting applications. As expected from the perfluorinated molecular structure and the amorphous nature, Cytop has been reported to have no absorption peaks between 1.0 and 2.5 μm.[26] However, its low T_g may not be suitable for waveguide applications for integrated optics. On the other hand, the T_g and the refractive index of Teflon-AF can be controlled by changing the copolymer ratio: decreasing the tetrafluoroethylene content increases the T_g over 300°C. In addition, its low dielectric constant and high chemical

Table 14.1. Molecular Structure and Properties of Amorphous and Semicrystalline Perfluoropolymers

Perfluoropolymer	Teflon AF	Cytop	PTFE
Morphology	Amorphous	Amorphous	Semicrystalline
Fluorine content (wt%)	67.1, 65.0	67.9	76.0
Glass transition temperature (°C)	160, 240a	108	—
Melting point (°C)	—	—	327
Dielectric constant	1.89–1.93	2.1–2.2	2.1
Refractive index	1.29–1.31	1.35	1.38
Optical transmittance (%) (visible region)	> 95	95	Opaque

a Glass transition temperature of no TFE content is higher than 300°C.

stability is preferable because optical waveguides are also used as insulating layers for electronic circuits in OEICs and OE-MCMs.

14.2. CHARACTERIZATION AND SYNTHESIS OF MATERIALS FOR PERFLUORINATED POLYIMIDES[27,28]

14.2.1. Reactivity Estimation of Perfluorinated Diamines

By petiuorination of polyimides, we expected to achieve not only low optical losses at 1.3 and 1.55 μm but also high thermal, chemical, and mechanical stability, low water absorption, and low dielectric constants. Perfluorinated polyimides can be synthesized from perfluorinated dianhydrides and diamines. Figure 14.3 lists a dianhydride and diamines that can be used for the synthesis of perfluorinated polyimides. Tetrafluoro-*p*-phenylenediamine (4FPPD), tetrafluoro-*m*-phenylenediamine (4FMPD), and 4,4'-diaminooctafluorobiphenyl (8BZ) are commercially available. Bis(2,3,5,6-tetrafluoro-4-aminophenyl)ether (8FODA) and bis(2,3,5,6-tetrafluoro-4-aminophenyl)sulfide (8FSDA) were prepared as described in the literature.[29,30] 1,4=Bis(trifluoromethyl)-2,3,5,6-benzenetetracarboxylic dianhydride (P6FDA) was the only previously known perfluorinated dianhydride that was synthesized in our laboratory.[31]

Fluorine is highly electronegative, which means that substituting it for hydrogen considerably decreases the acylation reactivity of the diamine monomers and increases the reactivity of the dianhydride monomers. Dine-Hart and Wright[32] synthesized a polyimide derived from PMDA and 8FBZ, but they could not obtain polymers with a high enough molecular weight for film formation.

To generate high-molecular-weight perfluorinated polyimides, it is first necessary to determine how fluorine affects the reactivity of the monomers. In particular, the effect of substituting hydrogen with fluorine on diamine reactivity is important because kinetic studies of the acylation of conventional monomers have revealed that acylation rate constants can differ by a factor of 100 among different dianhydrides, and by a factor of 10^5 among different diamines.[33]

To estimate the acylation reactivity of the perfluorinated diamines, poly(amic acid)s were prepared from the five diamines listed in Figure 14.3 and 6FDA dianhydride at room temperature. Equimolar amounts of dianhydride and diamine were added to *N,N*-dimethylacetamide (DMAc) to a concentration of 15 wt% and stirred at room temperature for 6 days under nitrogen. Table 14.2 shows the end-group content of the poly(amic acid)s determined from ^{19}F-NMR. 4FMPD shows the lowest end-group content, i.e., the highest reactivity, and 4FPPD shows the next highest. However, acylations were not complete for any of the diamines, and end-group contents were high even after 6 days of reaction at room temperature.
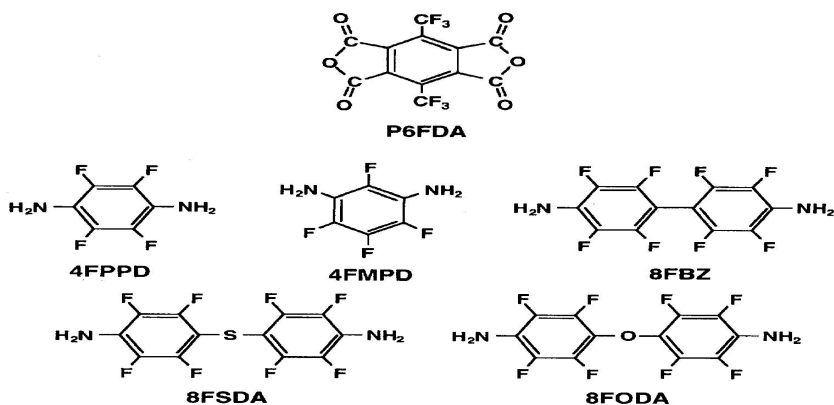
Figure 14.3. Structures of a dianhydride and diamines that can be used for perfluorinated polyimide synthesis (reproduced by permission of the American Chemical Society, from Ando *et al.*[28]).

When 8FBZ diamine, the least reactive one, was reacted with 6FDA, no NMR signal of the corresponding poly(amic acid) was detected.

   We reported the relationships between the NMR chemical shifts and the rate constants of acylation (k) as well as such electronic-property-related parameters as ionization potential (IP), electronic affinity (EA), and molecular orbital energy for a series of aromatic diamines and aromatic dianhydrides.[34] The usefulness of

Table 14.2. End-Group Contents of Poly(Amic Acid)s
Synthesized from Perfluorinated Diamines and 6FDA
Dianhydride

Diamine	End-group content (%)
4FPPD	42
4FMPD	15
8FODA	75
8FSDA	91
8FBZ	> 99

NMR chemical shifts for estimating the reactivity of polyimide monomers was first reported by Okude *et al.*[35] We revealed that the ^{15}N chemical shifts of the amino group of diamines (δ_N) depend monotonically on the logarithm of k (log k) and on IP. For the synthesis of perfluorinated polyimides, we attempted to estimate the reactivity of the five perfluorinated diamines from ^{15}N- and ^{1}H-NMR chemical shifts of the amino groups (δ_N and δ_H) and calculated IPs (IP$_{cal}$). Figure 14.4 plots δ_N against δ_H, with upfield displacement of chemical shifts (δ_N and δ_H are decreased) indicating the higher reactivity for acylation. The IP$_{cal}$ values calculated using MNDO-PM3 semiempirical molecular orbital theory[36] are also incorporated in the figure. From the δ_N, δ_H, and IP$_{cal}$ values of the diamines, 4FPPD is suggested to have the highest reactivity among the five, and 4FMPD is the next. However, this does not coincide with the end-group contents of poly(amic acid)s derived from the experiments described above. As shown in Figure 14.5, the acylation starts with a nucleophilic substitution in which diamine donates an electron to the dianhydride.[33] This reaction is called "first acylation" and it affords a monoacyl derivative (MAD). Poly(amic acid)s are generated by the
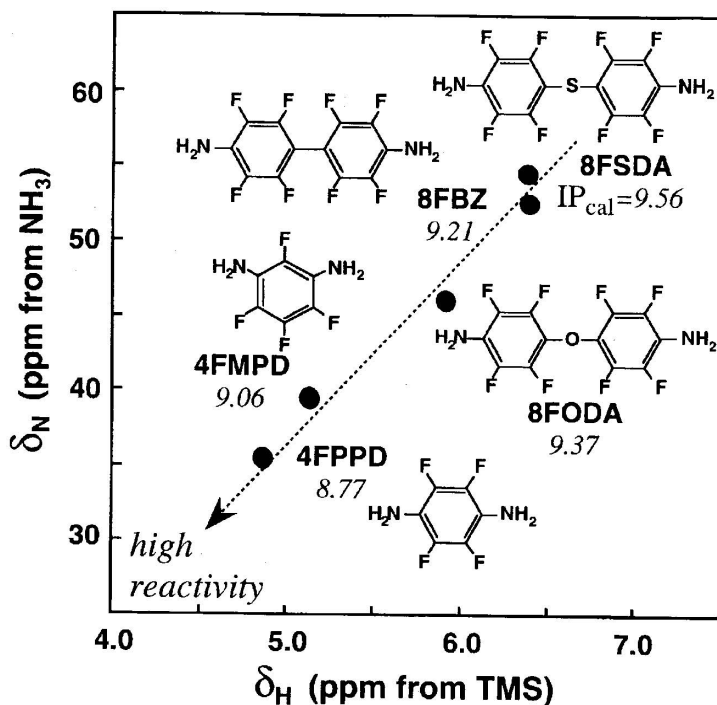

Figure 14.4. ^{15}N- and ^{1}H-NMR chemical shifts and calculated ionization potentials (eV) of perfluorinated diamines.
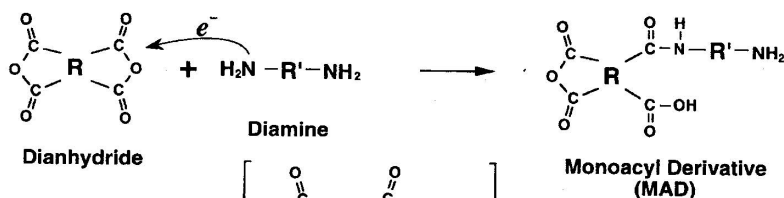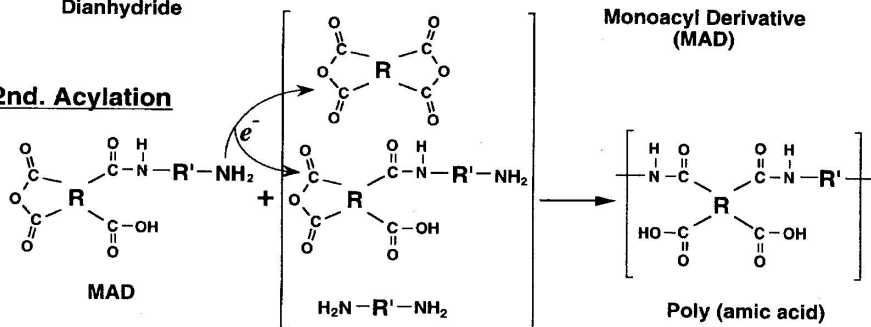
1st. Acylation

2nd. Acylation

Figure 14.5. Two-step acylation reactions that generate poly(amic acid) from diamine and tetra-carboxylic acid dianhydride (reproduced by permission of the American Chemical Society, from Ando *et al.*[28]) .

succeeding "second acylation," in which MAD reacts with dianhydride, diamine, or MAD. Therefore, the reactivity of MADs rather than that of diamines should be examined for synthesizing high-molecular-weight poly(amic acid)s.

The five perfluorinated diamines were reacted with equimolar amounts of phthalic anhydride in tetrahydrofuran to estimate their MAD reactivity. The molecular structures, δ_N, and δ_H of the diamines and the MADs are shown in Figure 14.6. The diamine of 8FBZ is not shown because no MAD could be obtained. The δ_N of 4FPPD was displaced downfield by 12.5 ppm in reacting to MAD that corresponds to a more than 10^3 decrease of acylation rate constant. On the other hand, the displacements of δ_N and δ_H for the other diamines are much smaller. This means that the reactivity of the residual amino group is little affected by the first acylation, unless two amino groups are located at the *para*-position in the same benzene ring. As a result, 4FMPD-MAD shows the highest reactivity coinciding with the result of the end-group content of poly(amic acid)s. Despite the fact that the δ_N and δ_H of 4FPPD-MAD are close to those of 8FODA-MAD, the end-group content of the poly(amic acid) derived from 4FPPD and 6FDA was lower than in the case of 8FODA and 6FDA. There may be some difference in the steric effects during the generation of poly(amic acid)s between one- and two-benzene ring diamines.
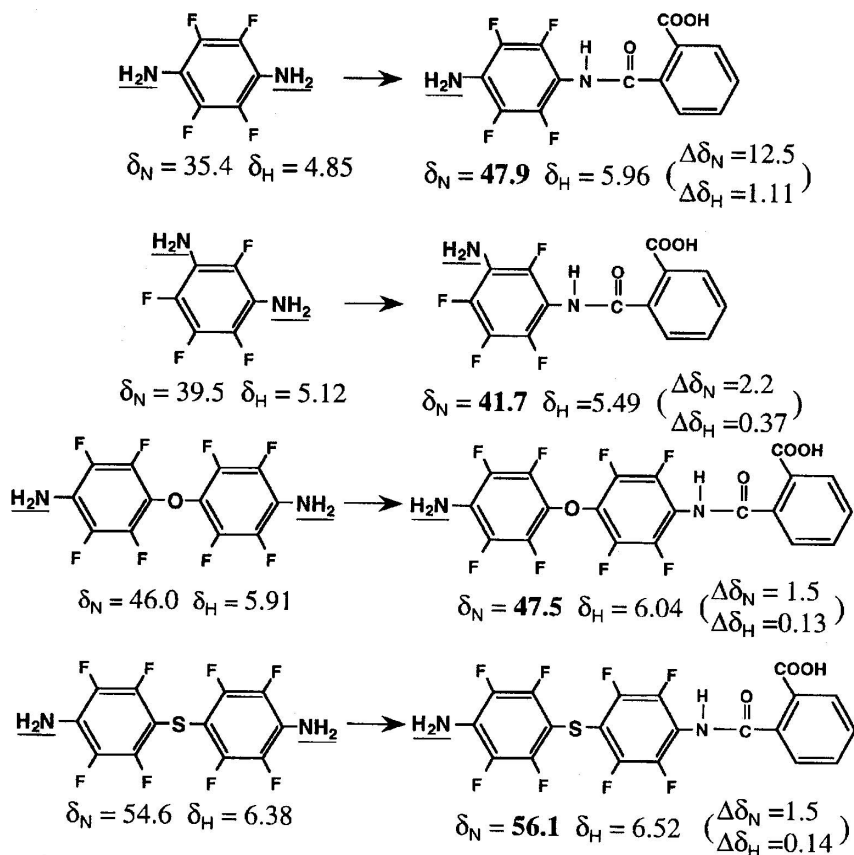
Figure 14.6. ^{15}N- and ^{1}H-NMR chemical shifts of perfluorinated diamines and their chemical shift changes caused by the first acylation (reproduced by permission of the American Chemical Society, from Ando et al.[28]).

Despite the difficulty noted above, Hougham et al.[37,38] succeeded in preparing continuous films from 4FPPD and 8FBZ as diamines and 6FDA as a dianhydride using skillful methods. They showed that two stages of polymerization are necessary to obtain high-molecular-weight polyimides from the perfluorinated diamines: a solution polycondensation at temperatures between 130 and 150°C followed by a high-temperature solid state chain extension of up to 350°C. FTIR spectra were measured for sequentially cured and cooled films of 6FDA/8FBZ, and they concluded that the chain extension begins at temperatures between 200 and 300°C; however, optimal mechanical properties were not realized with cure temperatures below 350°C. Using ^{13}C-NMR, we have observed

a similar phenomenon for a partially fluorinated 6FDA/TFDB polyimide dissolved in dimethylsulfoxide-d$_6$ (DMSO-d$_6$).[39] Hougham *et al.*[37] reported that increased fluorine in the polyimide backbone leads to a significant increase in the β-transition temperatures, and they suggested that a strong β-transition helps in polymerization in the solid.

14.2.2. Reactivity and Structural Problems of an Existing Perfluorinated Dianhydride

Because of the high electronegativity of fluorine, the introduction of fluorine or fluorinated groups into dianhydrides should increase the reactivity. Figure 14.7 shows structural formulas of conventional and fluorinated dianhydrides arranged in order of calculated electron affinity (EA$_{cal}$) using the MNDO-PM3 method and ^{13}C-NMR chemical shift of carbonyl carbons (δ$_C$).[40] The fluorinated dianhydrides in which trifluoromethyl (–CF$_3$) groups are directly bonded to benzene rings (P6FDA and P3FDA) are located rightmost with the largest EA$_{cal}$ values and the smallest δ$_C$, suggesting considerable increase in reactivity in the acylation reaction.[34] The EA$_{cal}$ of 6FDA, in contrast, is located between the unfluorinated PMDA and BPDA, and its δ$_C$ is larger than PMDA. This fact indicates that the reactivity enhancement caused by the introduction of a hexafluoroisopropylidene [–C(CF$_3$)$_2$ –]groupis not as high as that of a directly bonded –CF$_3$ group. This is because the electron-drawing effect of fluorines is blocked by the quaternary carbon. P6FDA is therefore expected to compensate for the low reactivity of perfluorinated diamines. However, the end-group content of the poly(amic acid) synthesized from 4FMPD and P6FDA was 36%, which is higher than that of poly(amic acid) prepared from 4FMPD and 6FDA. This reason is not clear; however a certain portion of anhydride rings might be open before the synthesis because this dianhydride is very sensitive to atmospheric moisture and moisture in the polymerization medium, although dianhydrides were sublimated under reduced pressure and all the synthesis procedures were carried out under nitrogen.

The resultant perfluorinated polyimide [PGFDA/4FMPD (**1**)] was cracked and brittle and did not form a continuous film. In the case of the other four
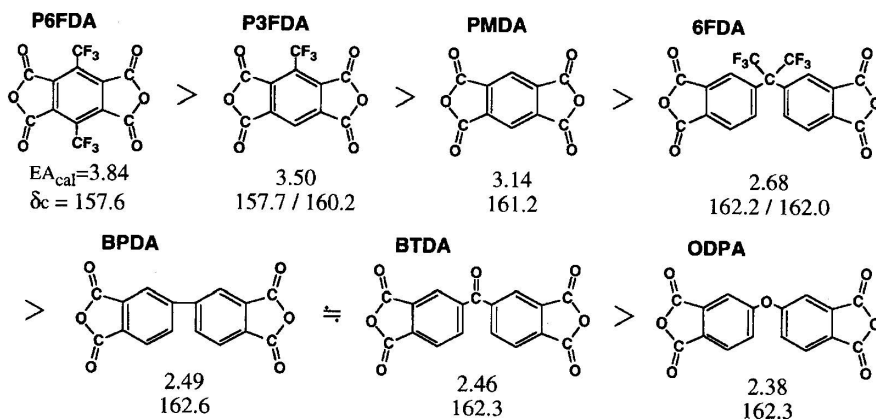

(1)

P6FDA/4FMPD
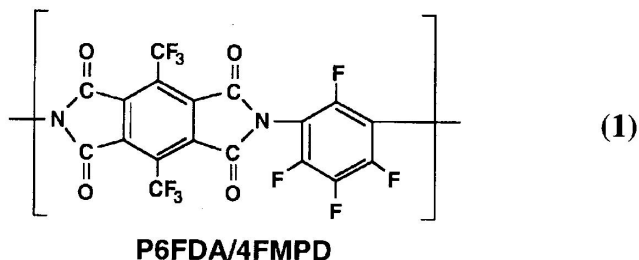
Figure 14.7. Aromatic dianhydrides arranged in order of calculated electron affinity (EA_{cal}) and ^{13}C-NMR chemical shift of carbonyl carbon (δ_C). Larger EA_{cal} and smaller δ_C correspond to the strong electron-accepting property of a dianhydride.

diamines, the polyimides prepared using P6FDA are coarse powder or films that have many cracks. One reason for the noncontinuous film is probably that the high reactivity of the per-fluorinated dianhydride could not compensate for the very low reactivity of perfluorinated diamines. However, the effect of the rigidity of the polyimide chain cannot be 'neglected in the cases of P6FDA and one-benzene-ring diamines. In this situation, bond rotation is permitted only at the imide linkage (nitrogen-aromatic carbon bonds). However, this rotation is restricted by steric hindrance between the fluorine atoms and carbonyl oxygens. Despite the bent structure at the *meta*-linkage of 4FMPD, the main chain of this polyimide should be very rigid. As Hougham *et al.*[37,38] have pointed out, a high-temperature solid state chain extension should take place for the formation of high-molecular-weight polyimides. However, this process accompanies conformational changes and molecular reorientation of polyimides. The chain extension reaction should be seriously impeded by the rigid molecular structure of PGFDA/4FMPD.

14.2.3. Synthesis of a Novel Perfluorinated Dianhydride

The lack of flexibility of the polymer chain has to be improved by introducing linkage groups into the dianhydride component. Accordingly, continuous and flexible films of perfluorinated polyimides are expected to be obtained by combining diamines, which have high reactivities, with dianhydrides, which have flexible molecular structures.

A novel perfluorinated dianhydride, 1,4-bis(3,4-dicarboxytrifluorophenoxy)-tetrafluorobenzene dianhydride (10FEDA), was synthesized according to Scheme

1. It should be noted that this molecule has two ether linkages that give flexibility to the molecular structure. In addition, the bulky –CF$_3$ groups in P6FDA are replaced by fluorine atoms. The δ_C of 10FEDA (157.5 ppm from TMS) was almost the same as that of P6FDA (157.6 ppm), so this dianhydride should have higher reactivity than unfluorinated and partially fluorinated dianhydrides.

14.3. SYNTHESIS AND CHARACTERIZATION OF PERFLUORINATED POLYIMIDES

14.3.1. Synthesis of Perfluorinated Polyimide (10FEDA/4FMPD)

To prepare the poly(amic acid), equimolar amounts of 10FEDA and 4FMPD were added to DMAc to a concentration of 15 wt% and stirred at room
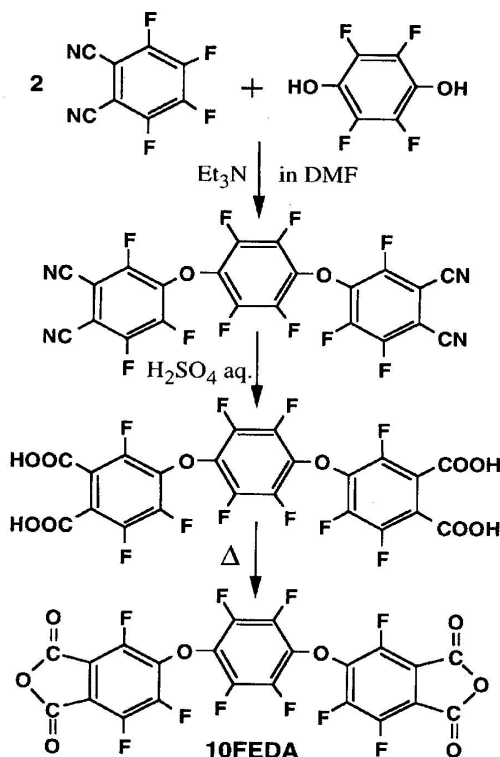
Scheme 1. Synthesis of 10EDA dianhydride.

temperature for 7 days under nitrogen. The end-group content of the poly(amic acid) estimated from ^{19}F-NMR was 6%, which is much less than that of P6FDA/4FMPD poly(amic acid) (36%). This is possibly due to the considerable increase in the flexibility of the dianhydride structure and the substitution of $-CF_3$ groups for fluorines. The poly(amic acid) derived from PGFDA is thought to have more structural distortion than that from 10FEDA because the molecular conformation around the amide group in the former is more restricted than in the latter by the steric hindrance between the bulky $-CF_3$ group and carbonyl oxygens.

The solution of poly(amic acid) was spin-coated onto a silicon wafer and heated first at 70°C for 2 h, at 160°C for 1 h, at 250°C for 30 mins, and finally at 350°C for 1h (Scheme 2). The resultant perfluorinated polyimide [10FEDA/4FMPD (**2**)] was a 9.5-μm-thick, strong, flexible film, pale yellow in color like conventional unfluorinated polyimides. The chemical formula of the 10FEDA/4FMPD polyimide was confirmed by elemental analysis. The fully cured film was not soluble in polar organic solvents, such as acetone, DMAc (DMF), and *N,N*-dimethylformamide. Thermal mechanical analysis (TMA) showed that the glass transition temperature was 309°C (Figure 14.8), which is about 30°C higher than the soldering temperature. Thermal gravimetric analysis (TGA) showed the initial polymer decomposition temperature to be 407°C. The dielectric constant was 2.8 at 1kHz.
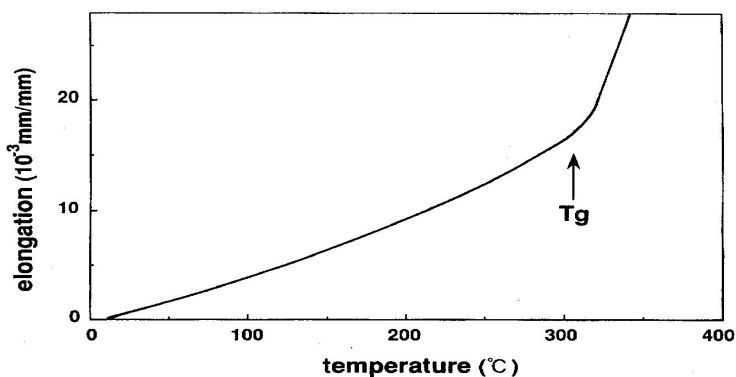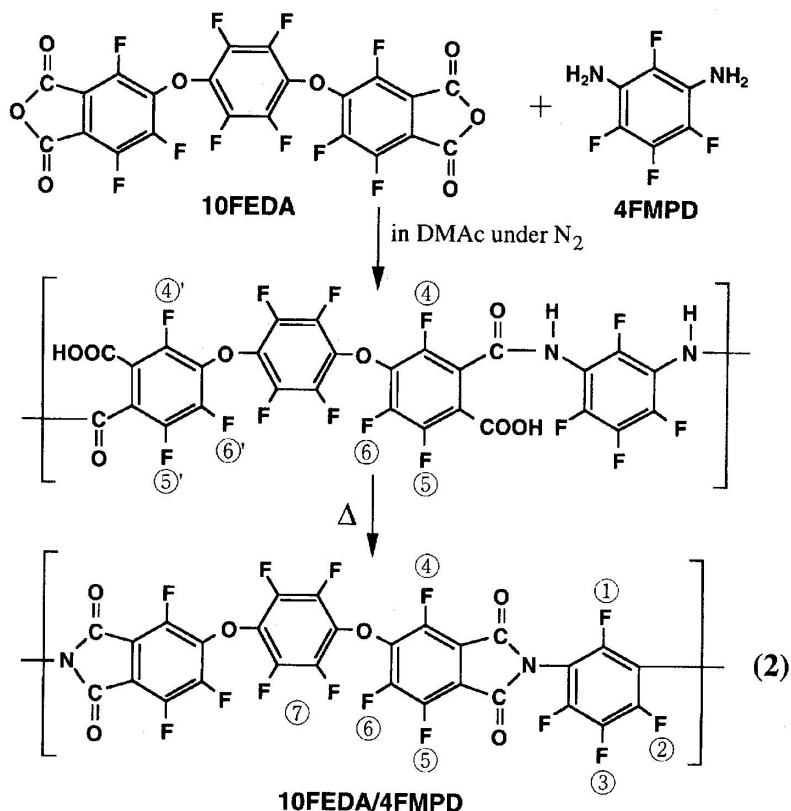

Figure 14.8. Thermal mechanical analysis (TMA) curve of 10FEDA/4FMPD film cured at 350°C (reproduced by permission of the American Chemical Society, from Ando *et al.*[28]) .

Scheme 2. Synthesis of 10FEDA/4FMPD polyimide.

14.3.2. Imidization Process Estimated from NMR and IR Spectra

Despite the insolubility of fully cured perfluorinated polyimide, the 10FEDA/4FMPD films cured below 200°C are soluble in polar organic solvents. The same phenomena have been observed for partially fluorinated polyimides.[40] Figure 14.9 shows the ^{19}F-NMR spectra of 10FEDA/4FMPD prepared at the final curing temperatures of 70, 120, 150, and 200°C. They were dissolved to a concentration of 5 wt% in DMSO-d_6. The signals in the spectra were assigned by using substituent effects determined from model compounds.[41] It is noteworthy that the signals assigned to the end groups of poly(amic acid) and/or polyimide are observed in all the NMR spectra. The terminal structures with amino groups of poly(amic acid) and polyimide are shown in Figure 14.10. The symbols of the peaks in Figure 14.9 correspond to the fluorines in Scheme 1 and Figure 14.10. The end-group contents determined from the intensity ratios of signal *c* (assigned
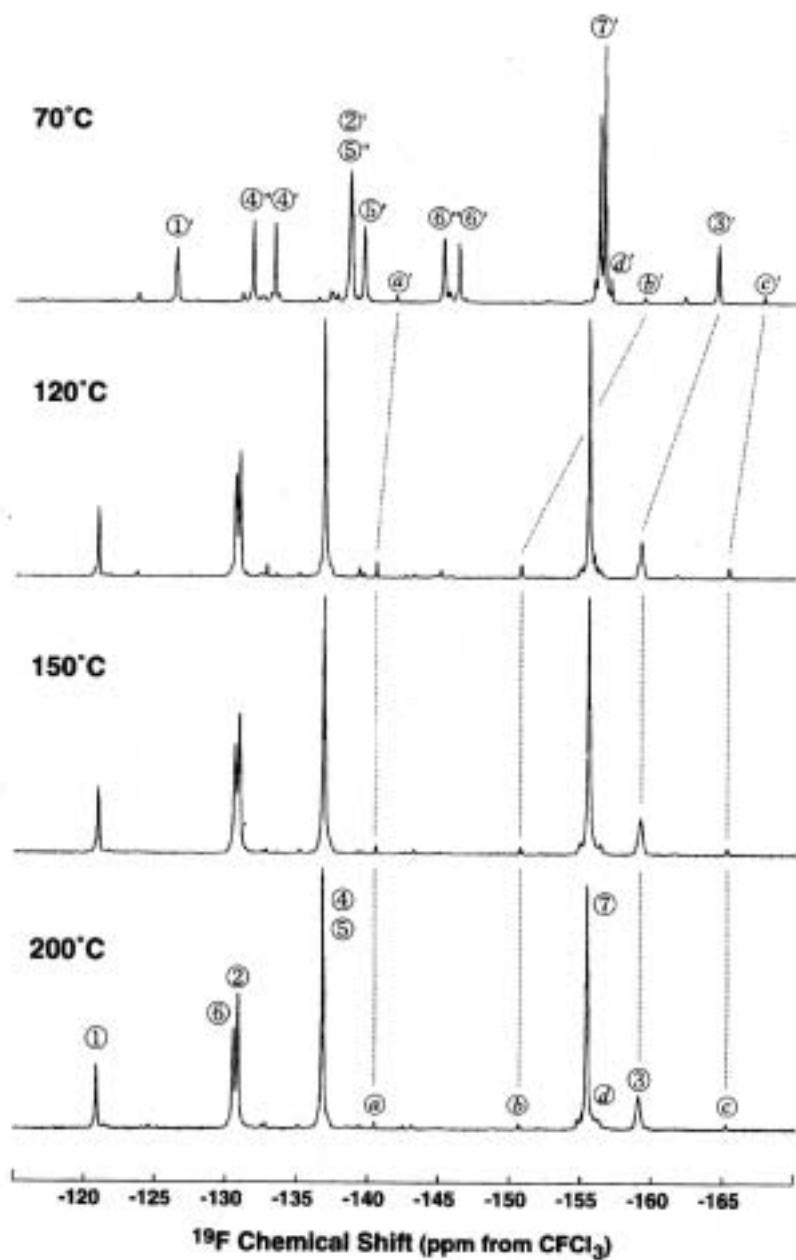
Figure 14.9. ^{19}F-NMR spectra of 10FEDA/4FMPD cured in nitrogen to 70, 120, 150, and 200°C dissolved in dimethylsulfoxide-d$_6$ (the numbering of peaks corresponds to the fluorines in Scheme 2 and Figure 14.10.

to the end-group) to signal 3 (assigned to the inner part of the polymer chain) are 8%, 15%, 9%, and 6% for 10FEDA/4FMPD cured at 70, 120, 150, and 200°C, respectively. This indicates that the degree of polymerization of the 120°C sample is smaller than that of PAA, suggesting that a depolymerization reaction occurs at amide groups of PAA at around 120°C. However, this low-molecular-weight polymer is gradually converted into a higher-molecular-weight polyimide by subsequent curing at higher temperatures (150 ~ 200°C) because the end-group content decreases with increasing curing temperature. As Hougham *et al.*[37,38] and the authors[39] have confirmed for partially fluorinated polyimides, condensation of the unreacted end groups of perfluorinated polyimides took place in the subsequent high-temperature curing between 200 and 350°C. The difference in solubility between the polyimides cured at 200 and 350°C can be explained by this chain extension reaction and by increased aggregation of the polyimide molecules with curing above T_g.

The NMR spectra in Figure 14.9 indicate that the imidization reaction began at 70°C and was completed at 150°C for 10FEDA/4FMPD. A ^{13}C-NMR examination of 6FDA/TFDB polyimide (3), in contrast, showed that the imidization became significant at 120°C and was complete at 200°C.[39] The imidization reaction of 10FEDA/4FMPD occurred at lower temperatures than 6FDA/TFDB. This can be explained by the higher electron-accepting properties and more flexible structure of 10FEDA compared to 6FDA.

The IR spectra of 6FDA/TFDB and 10FEDA/4FMPD cured at three final curing temperatures are shown in Figure 14.11. These spectra also confirm the NMR results. The absorption peaks specific to imide groups (1800 and 1750 cm^{-1}) are clearly seen in the 120°C sample of 10FEDA/4FMPD, and the spectrum is very similar to that of the fully cured polyimide at 350°C. On the other hand, the absorption peaks specific to the imide groups (1790 and 1740 cm^{-1}) can be observed for the 120°C sample of 6FDA/TFDB; however, the spectrum is much more similar to that of the 70°C sample in which most of the polymers have not been converted to polyimides.
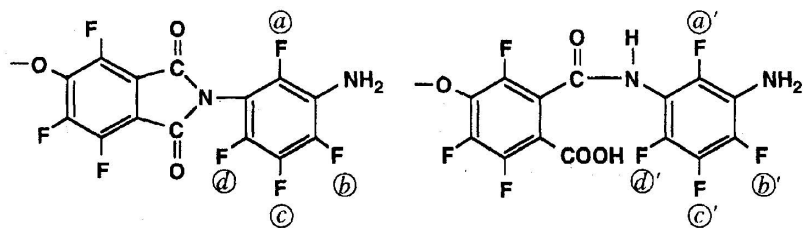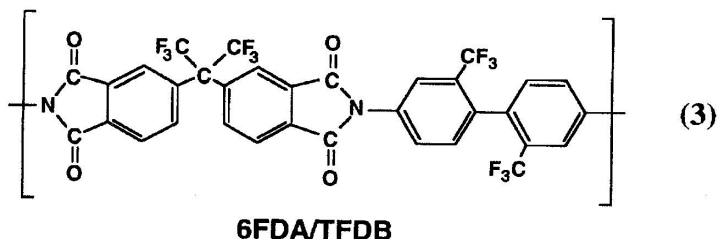

Figure 14.10. Amine-terminal structure of 10FEDA/4FMPD polyimide.

6FDA/TFDB

14.4. OPTICAL, PHYSICAL, AND ELECTRICAL PROPERTIES OF PERFLUORINATED POLYIMIDES

14.4.1. Optical Transparency at Near-IR and Visible Wavelengths

The near-IR absorption spectrum of 10FEDA/4FMPD film cured at 350°C is shown in Figure 14.12 together with that of partially fluorinated polyimide (6FDA/TFDB). The film thicknesses were about 25 μm. The perfluorinated polyimide has no substantial absorption peak over the wavelengths for optical communication except for a very small absorption peak at 1.5 μm that may be due to the fourth harmonic of the C=O stretching vibration of imide groups. Partially fluorinated polyimide, on the other hand, has an absorption peak due to the third harmonic of the stretching vibration of the C–H bond (1.1 μm), a peak due to the combination of the second harmonic of stretching vibration and deformation vibration of the C–H bond (1.4 μm), and a peak due to the second harmonic of the stretching vibration of the C–H bond (1.65 μm). Absorption peaks were assigned according to the peaks observed in PMMA.[21–23]

Figure 14.13 shows the UV-visible absorption spectra of perfluorinated (10FEDA/4FMPD), partially fluorinated (6FDA/TFDB), and unfluorinated [PMDA/ODA (4)] polyimides. The cut-off wavelengths (absorption edge, λ_0) of the absorption caused by electronic transition for 10FEDA/4FMPD (around 400nm) is located between those of 6FDA/TFDB and PMDA/ODA. This causes the yellowish color of 10FEDA/4FMPD. The coloration of polyimides is closely related to the extent of the charge transfer (CT) between alternating electron-donor (diamine) and electron-acceptor (dianhydride) moieties.[42] Kotov et al.[43] discussed the quantitative color changes in the polyimides derived from pyromellitic dianhydride from their λ_0s values in the optical absorption spectra. They found that the λ_0 is inversely correlated with the ionization potential of diamines and they attributed this mainly to the CT interaction. Reuter and Feger et al.[44–46] clarified that the optical losses in polyimides are caused by absorption that is due to the CT complexes and by scattering owing to ordering of the polyimide chains. The behavior of the optical losses at 830nm could not be predicted from that at 633 nm because the CT complexes absorption does not
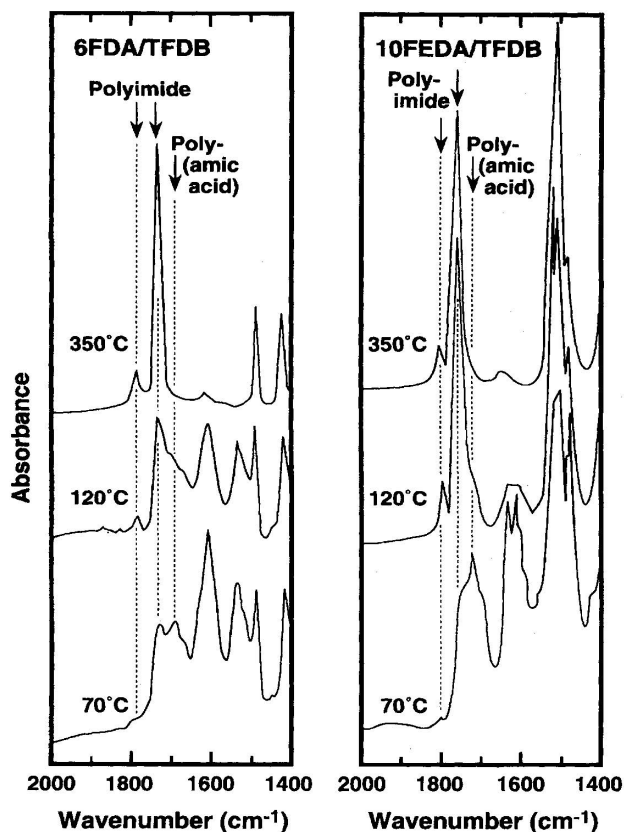
Figure 14.11. IR spectra of 6FDA/TFDB and 10FEDA/4FMPD cured in nitrogen to 70, 120, and 350°C.

affect the losses at 830 nm. They suggested that the chain ordering, which is the main cause of the optical losses at 830 nm, can be hindered sterically by the introduction of bulky side groups such as $-CF_3$ or $-C(CF_3)_2-$. The authors[40] have recently discussed the relationships between the color intensities of poly-imide films and the electronic properties of aromatic diamines and aromatic dianhydrides. The arrangement of the diamine moieties in the order of color intensity of the polyimides shows fairly good agreement with the order of the electron-donating properties of the diamines estimated from ^{15}N-NMR chemical shifts (δ_N). On the other hand, the arrangement of the dianhydride moieties in order of the color intensity of the polyimides agrees with the order of the electron-
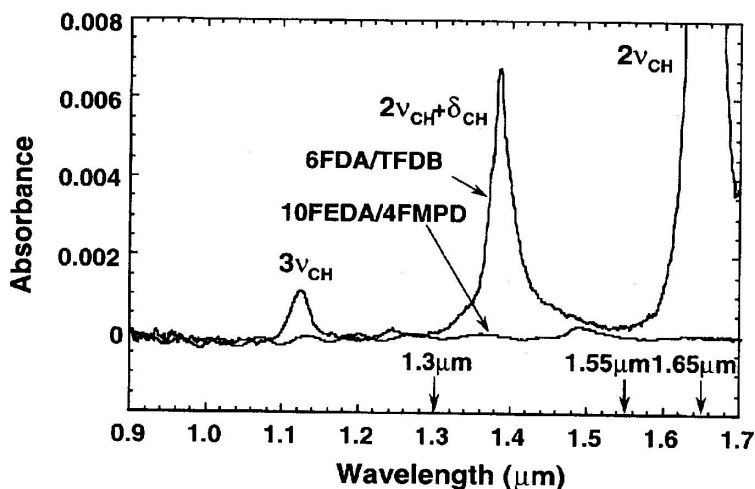
Figure 14.12. Visible–near-IR absorption spectra of 10FEDA/4FMPD and 6FDA/TFDB polyimide films.

accepting properties of the dianhydrides estimated from the experimental and calculated electron affinities. From this point of view, the coloration of perfluorinated polyimides is interesting because the polyimides are synthesized from the combination of the dianhydrides, having high-electron-accepting properties, and the diamines, having low-electron-donating properties. Although it is difficult to predict the color intensity of per-fluorinated polyimides from the combinations of dianhydrides and diamines, the λ_0 and yellowish color of 10FEDA/4FMPD indicate that the extent of the CT interaction of perfluorinated polyimide is stronger than that of partially fluorinated 6FDA/TFDB (no color) but slightly weaker than that of unfluorinated PMDA/ODA (pale yellow).
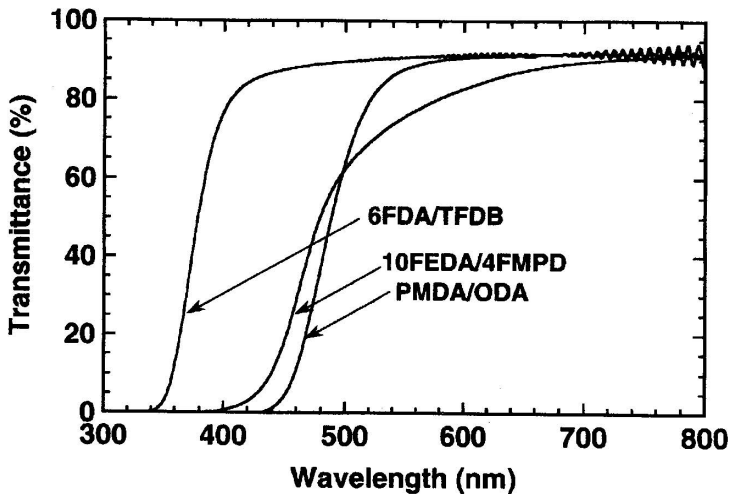

(4)
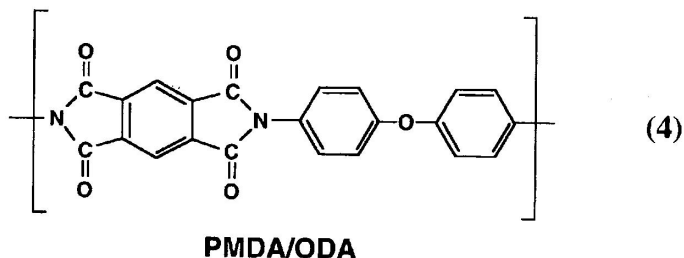
PMDA/ODA

Figure 14.13. UV–visible transmission spectra of partially fluorinated (6FDA/TFDB), perfluorinated (10FEDA/4FMPD), and unfluorinated polyimide (PMDA/ODA) films.

14.4.2. Mechanical Properties

Table 14.3 lists the strength and flexibility of perfluorinated polyimide films synthesized from the two dianhydrides and five diamines. Polymerizing 10FEDA with 8FODA or 8FSDA produced continuous, flexible films, but the films are slightly brittle compared with 10FEDA/4FMPD. As described above, P6FDA did not give any continuous films. Table 14.4 lists the mechanical properties of 10FEDA/4FMPD, 6FDA/TFDB, and PMDA/ODA.[47] All the films were prepared in our laboratory by spin-coating of poly(amic acid) on silicon substrates and cured at the highest temperature of 350°C under nitrogen. 10FEDA/4FMPD films have sufficient toughness for optical waveguide applications, and their mechanical properties are similar to those of 6FDA/TFDB; relatively higher tensile stress, higher elastic modulus, and lower elongation at break compared to PMDA/ODA.

14.4.3. Thermal, Electrical, and Optical Properties

Table 14.5 lists the thermal, electrical, and optical properties of perfluorinated polyimides, along with those of partially fluorinated and unfluorinated polyimides. Because of the flexible structure of the 10FEDA component, the polymer decomposition temperatures and T_g values of perfluorinated polyimides are slightly lower than those of conventional polyimides. This coincides with the results of Hougham *et al.*,[37] who reported that an increase in fluorine content in

Table 14.3. Strength and Flexibility of Perfluorinated Polyimide Films

Diamine	Dianhydride	
	10FEDA	P6FDA
4FPPD	–	No film
4FMPD	Strong and flexible	Brittle and cracked
8FODA	Flexible	No film
8FSDA	Flexible	No film
8FBZ	No film	No film

Table 14.4. Mechanical Properties of Perfluorinated (10FEDA/4FMPD), Partially Fluorinated (6FDA/TFDB), and Unfluorinated (PMDA/ODA) Polyimide Films[a]

Polyimide	Final cure temperature (°C)	Tensile strength (kgf/mm²)	5% Tensile stress (kgf/mm²)	Elongation at break (%)	Elastic modulus (kgf/mm²)
10FEDA/4FMPD	350	13.2	10.3	9	248
6FDA/TFDB	350	12.5	11.4	9	303
PMDA/ODA	350	10.5	6.5	40	232

[a] All samples were prepared under the same conditions,

the polyimide backbone led to only slight overall decrease in T_g but had little effect on dynamic thermal or thermooxidative stability. The thermal stability of these films is nonetheless high enough to withstand the manufacturing process for IC's and multichip modules. In addition, the direct introduction of fluorines into the aromatic rings does not cause a significant increase in fluorine content.

The adhesiveness of the perfluorinated polyimides is thus equivalent to that of partially fluorinated polyimides used for single-mode waveguide fabrications. Their dielectric constants (ε) at 1 kHz and average refractive indexes are as low as those of the partially fluorinated polyimides. This is primarily because the fluorine content of perfluorinated polyimides is comparable to that of partially fluorinated polyimides. Hougham *et al.*[38,48,49] investigated the fluorination effect on dielectric constants and refractive indexes for a series of polyimides. They assigned the observed decrease in relative permittivity and refractive index caused by fluorine substitution to effects of local electronic polarization and fractional free volume. The free-volume contribution was found to range from 25% for the polyimides with planer diamines to 94% for the polyimides with –CH₃ and very bulky –CF₃ groups.[49] Taking into account their elucidation, one finds that the similarity of dielectric constants and refractive indexes of perfluorinated polyimides to partially fluorinated polyimides with TFDB diamine is not straightforward because the

Table 14.5. Thermal, Electrical, and Optical Properties of Perfluorinated, Partially
Fluorinated, and Unfluorinated Polyimides

	Fluorine content (%)	Decomp. temperature (°C)	Glass transition temperature (°C)	Dielectric constant (ε)	Average refractive index ($\bar{n}$)	In-plane/out-of-plane birefringence ($\Delta n_\perp$)
10EDA/4FMPD	36.6	501	309	2.8	1.562	0.004
10FEDA/8FODA	38.4	485	300	2.6	1.552	0.004
10FEDA/8FSDA	37.7	488	278	2.6	1.560	0.006
10FEDA/TFDB	35.1	543	312	2.8	1.569	0.009
6FDA/TFDB	31.3	553	327	2.8	1.548	0.006
PMDA/TFDB	22.7	613	> 400	3.2	1.608	0.136
PMDA/ODA	0	608	> 400	3.5	1.714	0.088

former has a planer diamine structure and no $-CF_3$ group while the latter has at
least two $-CF_3$ groups.

It is worth noting that the in-plane/out-of-plane birefringence $(\Delta n_\perp)$* of
perfluorinated polyimides is lower than the partially fluorinated polyimides with
TFDB diamine. The low birefiingence is convenient for designing waveguide
structures in OEICs and in OE-MCM interconnections and for reducing polariza-
tion dependence of the optical waveguide circuits. Reuter *et al.*[14] reported that a
very low $\Delta n_\perp$ of 0.0034 at 633 nm was obtained by introducing two $-C(CF_3)_2-$
groups and a *meta*-phenylene linkage into the polyimide main chain. The
authors[50] reported that the conformational energy map calculated for decafluoro-
diphenylether $(C_6F_5-O-C_6F_5)$ using the MMP2 method is more similar to the
energy distribution of 2,2-diphenylhexafluoropropane $(C_6H_5-C(CF_3)_2-C_6H_5)$
than that of diphenylether $(C_6H_5-O-C_6H_5)$. Although the perfluorinated
phenyl rings can rotate around the ether linkage, decafluorodiphenylether shows
a much smaller low-energy region than diphenylether, and its optimum geometry,
i.e., a twist conformation, is the same as that of 2,2-diphenylhexafluoropropane.
Hence the low birefringence of per-fluorinated polyimides synthesized in this study
originates from the steric effect between perfluorinated aromatic rings and from a
number of bent structures such as ether, thioether, and *meta*-phenylene linkages.

These characteristics show that perfluorinated polyimides are promising
materials for waveguides in integrated optics and optical interconnect technology.
The thermal, mechanical, and optical properties of perfluorinated polyimides can
be controlled by copolymerization in the same manner as partially fluorinated
polyimides.[19]

*In-plane/out-of-plane birefringence $(\Delta n_\perp)$ is defined in this volume Ch. 15.

14.5. CONCLUDING REMARKS

Novel polymeric materials, 10FEDA/4FMPD, 10FEDA/8FODA, and 10FEDA/8FSDA perfluorinated polyimides, were synthesized. These materials can withstand soldering (270°C) and are highly transparent at the wavelengths of optical communications (1.0–1.7 μm). To generate high-molecular-weight perfluorinated poly(amic acid)s, the reactivities of five diamines and their monoacyl derivatives were estimated from the end-group contents of the corresponding poly(amic acid), ^{15}N- and ^{1}H-NMR chemical shifts, and calculated ionization potentials. A new perfluorinated dianhydride, 10FEDA, that has two ether linkages was synthesized in order to provide flexibility to the polymer chain. The perfluorinated polyimides prepared from 10FEDA dianhydride gave flexible films with T_g values over 270°C and high optical transparency over the entire optical communication wavelength range with sufficient mechanical strength. In addition, their dielectric constants and refractive indexes are as low as those of conventional fluorinated polyimides, and their in-plane/out-of-plane birefringence is low. These characteristics indicate that perfluorinated polyimides are promising materials for optical communication applications.

14.6. REFERENCES

1. Y. Suematsu and K. Iga, *Introduction to Optical Fiber Communications,* John Wiley and Sons, New York (1982), 208 pp.
2. I. Sankawa, S. Furukawa, Y. Koyamada, and H. Izumita, *IEEE Photon. Technol. Lett. 2,* 766–768 (1990).
3. H. Yokota, H. Kanamori, Y. Ishiguro, and H. Shinba, *Technical Digest of Optical Fibers Conference '86* (Atlanta), Conference on Optical Fiber Communication, Washington D.C. (1986), Postdeadline Paper 3.
4. T. Miya, Y. Terunuma, T. Hosaka, and T. Miyashita, *Electron. Lett. 15,* 106–108 (1979).
5. S. E. Miller, *Bell. Syst. Tech. J. 48,* 2059–2069 (1969).
6. J. W. Goodman, F. J. Leonberger, S. Kung, and R. Athale, *Proc. IEEE. 72,* 850 (1984).
7. M. Seki, R. Sugawara, H. Hashizume, and E. Okuda, *Proceedings of the Optical Fibers Conference '89* (Houston), Conference on Optical Fiber Communication, Washington D.C. (1989), Postdeadline Paper 4.
8. M. Kawachi, M. Kobayashi, and T. Miyashita, *Proceeding of the European Conference on Optical Fiber Communication '87* (Helsinki), Consulting Committee of the Professional Electroengineers Organization, Helsinki, Finland (1987), p. 53.
9. T. Kurokawa, N. Takato, and T. Katayama, *Appl. Opt. 19,* 3124–3129 (1380).
10. K. Furuya, B. I. Miller, L. A. Coldman, and R. E. Howard, *Electron. Lett. 18,* 204–205 (1982).
11. H. Franke and J. D. Crow, in *Integrated Optical Circuit Engineering III* (R. T. Kersten, ed.), *Proc. Soc. Photo-Opt. Instrum. Eng. 651,* 102 (1986).
12. C. T. Sullivan, in *Optoelectronic Materials, Devices, Packaging, and Interconnects II* (G. M. McWright and H. J. Wojtunik, eds.), *Proc. Soc. Photo-Opt. Instrum. Eng. 994,* 92–100 (1988).

13. J. M. Hagerhorst-Trewhella, J. D. Gelorme, B. Fan, A. Speth, D. Flagello, and M. M. Optysko, in *Integrated Optics and Optoelectronics* (K. K. Wong, H. J. Wojtunik, S. T. Peng, M. A. Mentzer, and L. McCaughan, eds.), *Proc. Soc. Photo-Opt. Instrum. Eng. 1177,* 379–386 (1989).

14. R. Reuter, H. Franke, and C. Feger, *Appl. Opt. 27,* 4565–4571 (1988).

15. T. Matsuura, S. Ando, S. Matsui, S. Sasaki, and S. Yamamoto, *Electron. Lett. 29,* 2107–2109 (1993).

16. T. Maruno, T. Matsuura, S. Ando, and S. Sasaki, *Nonlin. Opt. 15,* 485–488 (1996).

17. J. Kobayashi, T. Matsuura, S. Sasaki, and T. Maruno, *Appl. Opt 37,* (6), 1032–1037 (1998).

18. T. Matsuura, Y. Hasuda, S. Nishi, and N. Yamada, *Macromolecules 24,* 5001–5005 (1991).

19. T. Matsuura, S. Ando, S. Sasaki, and F. Yamamoto, *Macromolecules 27,* 6665–6670 (1994).

20. Product Bulletin H-1A, E.I. du Pont de Nemours and Company.

21. W. Groh, *Makromol. Chem. 189,* 2861–2874 (1988).

22. T. Kaino, M. Fujiki, and S. Nara, *J. Appl. Phys. 52,* 7061–7063 (1981).

23. T. Kaino, K. Jinguji, and S. Nara, *Appl. Phys. Lett. 42,* 567–569 (1983).

24. S. Imamura, R. Yoshimura, and T. Izawa, *Electron. Lett. 27,* 1342 (1991).

25. F. Yamamoto, I. Sankawa, S. Furukawa, and Y. Koyamada, *IEEE Photonics Tech. Lett. 4,* 1392–1394 (1992).

26. K. Aosaki, *Plastics (Japan) 42,* 51–56 (1991).

27. S. Ando, T. Matsuura, and S. Sasaki, *Macromolecules 25,* 5858–5860 (1992).

28. S. Ando, T. Matsuura, and S. Sasaki, in *Polymers for Microelectronics, Resists and Dielectrics* (L. F. Thompson, V. G. Willson, and S. Tagawa, eds.), ACS Symposium Series 537, American Chemical Society, Washington, DC. (1994), pp. 304–322.

29. I. L. Knunyants and G. G. Yakobson, *Syntheses of Fluoroorganic Compounds,* Springer-Verlag, Berlin (1985), pp. 197–198 [Original paper: L. S. Kobrina, G. G. Furin, and G. G. Yakobsen, *Zh. Obshch. Khim. 38,* 514 (1968) (in Russian)].

30. I. L. Knunyants and G. G. Yakobson, *Syntheses of Fluoroorganic Compounds,* Springer-Verlag, Berlin (1985), pp. 196–197 [Original paper: G. G. Furin, S. A. Kurupoder, and G. G. Yakobsen, *IIzv. Sib. Otd. Akad. Nauk. SSSR Ser. Khim. Nauk 5,* 146 (1976) (in Russian)].

31. T. Matsuura, M. Ishizawa, Y. Hasuda, and S. Nishi, *Macromolecules 25,* 3540–3544 (1992).

32. R. A. Dine-Hart and W. W. Wright, *Makromol. Chem. 153,* 237–254 (1972).

33. M. I. Bessonov, M. M. Koton, V. V. Kudryavtsev, and L. A. Laius, *Polyimides: Thermally Stable Polymers,* Consultants Bureau, New York (1987), Ch. 2.

34. S. Ando, T. Matsuura, and S. Sasaki, *J. Polym. Sci. Pt. A: Polym. Chem. 30,* 2285–2293 (1992).

35. K. Okude, T. Miwa, K. Tochigi, and H. Shimanoki, *Polym. Preprints 32,* 61–62 (1991).

36. J. J. P. Stewart, *J. Computational Chem. 10,* 209–220 (1989), and the program used is MOPAC Ver.6.0 [J. J. P. Stewart, Quantum Chemistry Program Exchange #455, *QCPE Bull. 9,* 10 (1989)].

37. G. Hougham, G. Tesoro, and J. Shaw, in *Polyimides, Materials, Chemistry and Characterization* (C. Feger, M. M. Khojasteh, J. E. McGrath, eds.), Elsevier Science, Amsterdam (1989), p. 465.

38. G. Hougham, G. Tesoro, and J. Shaw, *Macromolecules 27,* 3642–3649 (1994).

39. S. Ando, T. Matsuura, and S. Nishi, *Polymer 33,* 2934–2939 (1992).

40. S. Ando, T. Matsuura, and S. Sasaki, *Polym. J. 29,* 69–74 (1997).

41. S. Ando and T. Matsuura, *Mag. Res. Chem. 33,* 639–645 (1995).

42. R. A. Dine-Hart and W. W. Wright, *Makromol. Chem. 143,* 189–206 (1972).

43. B. V. Kotov, T. A. Gordina, V. S. Voishchev, O. V. Kolninov, and A. N. Pravednikov, *Vysokomol. Soyed. A19,* 614 (1977).

44. R. Reuter and C. Feger, *SPE Tech. Paper 36,* 889–892 (1990).

45. R. Reuter and C. Feger, *SPE Tech. Paper 37,* 1594–1597 (1991).

46. C. Feger, S. Perutz, R. Reuter, J. E. McGrath, M. Osterfeld, and H. Franke, in *Polymeric Materials for Microelectronic Applications* (H. Ito, S. Tagawa, and K. Horie, eds.), *ACS Symp. Ser. 579;* American Chemical Society: Washington, D.C. (1994), pp. 272–282.

47. T. Matsuura, S. Ando, and S. Sasaki, unpublished results (1996).
48. G. Hougham, G. Tesoro, A. Viehbeck, and J. D. Chapple-Sokol, *Macromolecules 27,* 5964–5971 (1994).
49. G. Hougham, G. Tesoro, and A. Viehbeck, *Macromolecules 29,* 3453–3456 (1996).
50. S. Ando, T. Matsuura, and S. Sasaki, *Polym. Preprints Jpn. 41,* 957 (1992).